Received 3 December 2020; revised 22 January 2021; accepted 25 January 2021. Date of publication 8 February 2021; date of current version 2 March 2021.

Digital Object Identifier 10.1109/OJAP.2021.3057138

Electromagnetic Scattering by Metallic Targets Above a Biological Medium With a Spectral-Domain Approach

CRISTINA PONTI [1,2] (Member, IEEE), LUDOVICA TOGNOLATTI [1,2] (Graduate Student Member, IEEE), AND GIUSEPPE SCHETTINI [1,2] (Senior Member, IEEE)

[1]Department of Engineering, Roma Tre University, 00146 Rome, Italy
[2]National Interuniversity Consortium for Telecommunications, Roma Tre University, 00146 Rome, Italy

CORRESPONDING AUTHOR: C. PONTI (e-mail: cristina.ponti@uniroma3.it)

This work was supported in part by the Italian Ministry for Education, University, and Research through the Project PRIN2017 "WPT4WID: Wireless Power Transfer for Wearable and Implantable Devices," under Grant 2017YJE9XK.

ABSTRACT The scattering of a far-field source by perfectly conducting targets above a semi-infinite lossy medium is studied. An analytical solution is applied to the electromagnetic scattering problem with the Cylindrical Wave Approach. Interaction of a plane-wave field with the cylindrical targets is expressed through expansions into cylindrical waves, and a spectral approach is used to deal with the interaction of the scattered field and the interface. The method allows modelling the interaction of an external source with a biological medium, in the presence of external metallic objects. In the numerical examples, the electrical parameters of a muscle are used to model the biological tissue. Application to cases of interest for the total field transmitted in the muscle is investigated for both TM and TE polarization states. Penetration of the electromagnetic field is evaluated, both at the ISM frequency of 2.4 GHz and in the millimeter frequency range at 28 GHz.

INDEX TERMS Electromagnetic scattering, electromagnetic propagation in absorbing media, biological tissues.

I. INTRODUCTION

EMERGING research in the field of implantable antennas for continuous wireless health control of patients is motivated by promising advantages in terms of social and economic impact [1]–[3]. Choice of the operational frequency is a crucial point, due to considerations on size of the devices as well as attenuation in human tissues and efficient antenna feeding. Usage of unlicensed Industrial, Scientific and Medical (ISM) bands at 2.4 or 5.8 GHz, of Wi-Fi or Bluetooth communication networks, offers moderately miniaturized devices but with a limited bandwidth availability [7]. In the frame of 5G communication systems, promising perspectives for body-centric wireless communications are given in the millimeter frequency bands, due to massive amount of bandwidth and potential multigigabit-per-second (Gb/s) data rates. At millimeter frequencies, researches are mostly pursued in the field of wearable devices [4] or new flexible and stretchable sensors directly attached to the human skin [6]. Development of implantable devices with millimeter waves is attractive but very challenging, because of the high absorption of the electromagnetic fields by the human tissues [5]. Due to the high path loss, millimeter wave links are also limited in range, and the effect of diffuse scattering by walls, and scattering patterns of common use objects in an indoor environment can be included, for a more accurate evaluation of the propagation in ray-tracing models [8]. From the point of view of clothing and garment materials, studies have assessed that attenuation of most fabrics is negligible [9], [10].

The role of small and unwanted objects that may be close to a wearable or implantable antenna, as neklaces, buckles or buttons, has not been explored, and it is subject of consideration in this article. In the frame of short-medium range wireless communication links, the work aims at providing

a tool useful to find the field scattered by small metallic targets, like buttons or other wearable objects, and partially transmitted to a receiving antenna placed inside, or inserted in close proximity to, an underlying human body here simulated by a biological medium. The whole system is excited by the far field radiation of an external feeding source. This is a problem that it is also of interest for wireless recharging of in-body electronic devices.

The problem is dealt with a two-dimensional approach, as the targets are modelled with circular cross-section cylinders of infinite length. They are placed in a background of two semi-infinite media, the one above filled with air, and containing both the cylinders and the plane-wave used as source of the scattering problem, and the lowest one filled by a dielectric medium with lossy dielectric permittivity, in order to model a biological tissue. In other advanced scattering applications, cylindrical targets need to be modelled in a scattering environment, which includes one or more planar discontinuities, with cylinders buried in the subsoil below an interface, as in the case of Ground Penetrating Radar (GPR) [11] applications, or placed below a dielectric slab, as in the Through-the-Wall radar modelling [12]. In these fields, different numerical techniques have been proposed, mainly based on integral equations, solved with Method of Moments [13]–[23]. As most of the targets can be approximated with circular cross-section cylinders, also analytical approaches, using expansions into cylindrical waves, and implemented through plane-wave spectra, have been developed [26]–[31]. In particular, a technique, called Cylindrical Wave Approach (CWA) has been proposed, to deal with scattering by cylinders buried in a semi-infinite medium below a flat interface [25], [26], or a rough one [27], [28], placed inside a dielectric slab [29], or hidden below a wall [30], [31]. Other interesting applications of scattering by buried targets are in the microwave imaging of biological tissues, as in the breast cancer imaging with microwave fields, that aims at detecting the dielectric contrast between malignant tumor and healthy breast tissue [32]. Another emerging field of application is relevant to brain stroke imaging and monitoring [33].

In the literature, the scattering layout dealt with in this article, with targets placed above an interface, has received less attention. An analytical method is proposed in [34], employing expansion in cylindrical waves; the scattered field by the targets is evaluated only in air, including the scattered-reflected field by the interface. The approach in [34] is here extended and implemented with the CWA, evaluating also the scattered-transmitted field in the lowest half-space. The expressions of the scattered fields are also dealing with a lossy medium filling the lower half-space, in order to model permittivity and electric conductivity of a biological tissue in the microwave frequency range.

This article is organized as follows: in Section II, the theoretical approach is presented; in Section III, validation of the method, and numerical results are given. Conclusions of the work are drawn in Section IV.

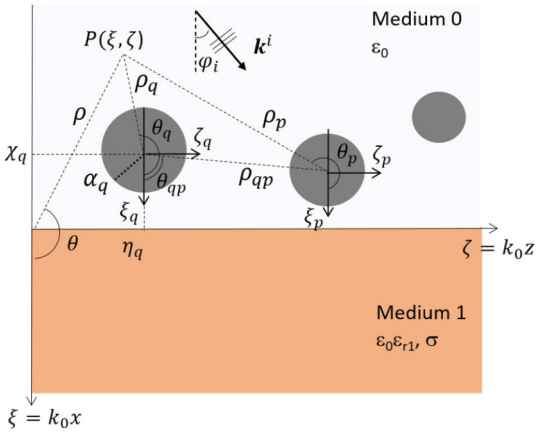

FIGURE 1. Geometry of the scattering problem.

II. THEORETICAL ANALYSIS

The geometry of the scattering problem is illustrated in Fig. 1. A two-dimensional problem with two half spaces separated by a flat interface is considered. The upper medium (Medium 0) is filled with air, characterized by vacuum-like permittivity ε_0, and the lowest one (Medium 1) is a lossy medium with real permittivity $\varepsilon_1 = \varepsilon_0\varepsilon_{r1}$ and conductivity σ, and it is linear, homogeneous, and isotropic. In Medium 0, above the separation interface, N perfectly conducting cylinders are placed, with parallel axes and parallel to the interface. A two-dimensional problem is considered, assuming that the structure has an infinite extension along the y-direction. A main reference frame *(MRF)* (O, ξ, ζ) of normalized coordinates $\xi = k_0 x$ and $\zeta = k_0 z$ is used, where $k_0 = \omega/c$ is the vacuum wavenumber. N reference frames RF_p centered on the axis of the p-*th* (p = 1,..., N) cylinder are also introduced, both referring to rectangular ($\mathrm{O_p}$, ξ_p, ζ_p) and polar ($\mathrm{O_p}$, ρ_p, θ_p), coordinates where $\xi_\mathrm{p} = k_0 x_\mathrm{p} = \xi - \chi_\mathrm{p}$, $\zeta_\mathrm{p} = k_0 z_\mathrm{p} = \zeta - \eta_\mathrm{p}$ and $\rho_\mathrm{p} = k_0 r_\mathrm{p}$. In *(MRF)* the p-*th* cylinder has centre in (χ_p, η_p), being $\chi_\mathrm{p} < 0$ the coordinate of the p-th cylinder along ξ, and $\alpha_\mathrm{p} = k_0 a_\mathrm{p}$ the normalized radius. The analysis is performed for a monocromatic source field, and the term $e^{-i\omega t}$ is omitted throughout the analysis.

The scattered field by the cylinders is solved implementing the CWA and extending the formulation proposed in [34], [35]. A scalar function $V(\xi, \zeta)$ is used to describe the y-directed electric field E, in case of $TM^{(\mathrm{y})}$ polarization, or the y-directed magnetic field H, in the $TE^{(\mathrm{y})}$ one. The source of the scattering problem is a plane-wave field V_i, propagating in Medium 0 and impinging towards the planar interface forming an angle φ_i with the positive direction of the ξ-axis. In the employed approach, the total field in each medium is decomposed in several field terms, as depicted in Fig. 2.

Decomposition of the total field in Medium 0 is applied, and it leads to the following contributions:

- $V_\mathrm{i}(\xi, \zeta)$: plane-wave incident field;
- $V_\mathrm{r}(\xi, \zeta)$: plane-wave reflected field, excited by reflection of the incident field V_i by the interface;

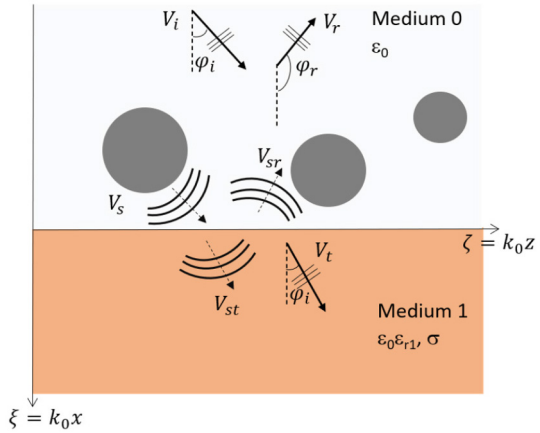

FIGURE 2. Decomposition of the total field.

- $V_s(\xi, \zeta)$: scattered field by the cylinders;
- $V_{sr}(\xi, \zeta)$: scattered-reflected field, excited by reflection of the scattered field V_s at the interface;

In this work, the perspective is on the field penetrating into Medium 1, in order to assess the amount of field transmitted below the interface. As field contributions in Medium 1, the following terms are detected:

- $V_t(\xi, \zeta)$: plane-wave transmitted field, excited by transmission of the incident field V_i through the interface;
- $V_{st}(\xi, \zeta)$: scattered-transmitted field, excited by transmission of the scattered field V_s through the interface;

The scattered-transmitted field V_{st} is derived with the CWA through an expansion into suitable cylindrical waves of m-*th* order. Preliminarily, the expression of the plane wave spectrum of a generic cylindrical function of order m is recalled [36], [37]:

$$CW_m(\xi, \zeta) = \frac{1}{2\pi}\int_{-\infty}^{+\infty} F_m(\xi, n_\parallel) e^{in_\parallel \zeta} dn_\parallel \tag{1}$$

where F_m is the angular spectrum of a cylindrical function, with explicit expression given by:

$$F_m(\xi, n_\parallel) = \frac{2}{\sqrt{1-(n_\parallel)^2}} e^{i|\xi|\sqrt{1-(n_\parallel)^2}} \times \begin{cases} e^{im \arccos n_\parallel}, \xi \geq 0 \\ e^{-im \arccos n_\parallel}, \xi \leq 0 \end{cases} \tag{2}$$

The definition (1) can be used as set of basis functions expressing the scattered field in Medium 0. Therefore, the relevant scattered field transmitted in Medium 1 can be found using, as basis functions, transmitted cylindrical waves derived from (1). The transmission coefficient $T_{01}(n_\parallel)$ from Medium 0 to Medium 1 is applied, and the propagation term of a generic transmitted plane wave is defined, through the normalized transmitted wavevector $\mathbf{k}^t/k_1 = \mathbf{n}^t = n_\perp^t \hat{\mathbf{x}} + n_\parallel^t \hat{\mathbf{z}}$, where k_1 is the modulus of $\mathbf{k}^t$, with $n_\parallel^t = n_\parallel/n_1$, and $n_\perp^t = \sqrt{1-(n_\parallel^t)^2}$. n_1 is the refraction index of Medium 1, which accounts for the losses and it is $n_1 = \sqrt{\varepsilon_{r1} + i\sigma/(\omega\varepsilon_0)}$. The final definition of the m-*th* order transmitted cylindrical wave is:

$$TW_m(\xi, \zeta; \chi_q) = \frac{1}{2\pi}\int_{-\infty}^{+\infty} T_{01}(n_\parallel) F_m(\chi_q, n_\parallel) \times e^{i\sqrt{1-(n_\parallel/n_1)^2}\xi} e^{in_\parallel(\zeta-\eta_q)} dn_\parallel \tag{3}$$

In Eqs. (1)-(3) real and imaginary parts of the square roots are assumed in such a way to fully respect Sommerfeld conditions for outgoing waves. Employing Eq. (3) as basis functions, the scattered-transmitted field V_{st}, as result of contribution by the N cylinders above the interface, can be written in the following form:

$$V_{st}(\xi, \zeta) = V_0 \sum_{q=1}^{N} \sum_{m=-\infty}^{+\infty} c_{qm} TW_m(\xi, \zeta; \chi_q) \tag{4}$$

The field in (4) is expressed through unknown expansion coefficients c_{qm}. They are computed by solving the scattering problem in Medium 0, following the formulation presented in [34], that is here briefly recalled.

The scattered field V_s, and the scattered reflected field V_{sr}, are expressed in a similar manner as expansions into cylindrical waves, through the same expansion coefficients c_{qm} used in (4) [34]. As to the scattered field V_s, the following expression in polar coordinates is employed, by applying the addition Theorem of Hankel functions [38]:

$$V_s(\xi, \zeta) = V_0 \sum_{\ell=-\infty}^{+\infty} J_\ell(\rho_p) e^{i\ell\theta_p} \sum_{q=1}^{N} \sum_{m=-\infty}^{+\infty} c_{qm} \times \left[CW_{m-\ell}(\xi_{qp}, \zeta_{qp})(1-\delta_{qp}) + \frac{H_\ell^{(1)}(\rho_p)}{J_\ell(\rho_p)} \delta_{qp}\delta_{\ell m} \right] \tag{5}$$

where CW_m is the m-*th* order cylindrical function defined in (1), which may be expressed, alternatively, through

$$CW_m = H_m^{(1)}(\rho_p) e^{ip\theta_p} \tag{6}$$

with $H_m^{(1)}(\rho_p)$ a first-kind Hankel function, and $e^{ip\theta_p}$ an angular term.

Reflected cylindrical waves of m-*th* order, RW_m, are employed as basis functions of the scattered-reflected field V_{sr}:

$$RW_m(\xi, \zeta) = \frac{1}{2\pi}\int_{-\infty}^{+\infty} \Gamma_{01}(n_\parallel) F_m(\xi, n_\parallel) e^{in_\parallel \zeta} dn_\parallel \tag{7}$$

where $\mathbf{n}^r = -n_\perp \hat{\mathbf{x}} + n_\parallel \hat{\mathbf{z}}$ is the normalized reflection wavevector, derived from the Snell's law, $\Gamma_{01}(n_\parallel)$ is the reflection coefficient, at the interface of separation between Medium 0 and Medium 1, and F_m is the plane-wave spectrum already introduced in (2). The scattered-reflected field V_{sr} in polar coordinates, through the (7), is defined as follows:

$$V_{sr}(\xi, \zeta) = V_0 \sum_{\ell=-\infty}^{+\infty} J_\ell(\rho_p) e^{i\ell\theta_p} \sum_{q=1}^{N} \sum_{m=-\infty}^{+\infty} c_{qm} \times RW_{m+\ell}(\chi_p + \chi_q, \eta_p - \eta_q) \tag{8}$$

The unknown scattered fields are found by imposing the boundary conditions at the cylinders' interface, for $TM^{(y)}$ and $TE^{(y)}$ polarizations, respectively.

$$[V_i + V_r + V_s + V_{sr}]_{\rho_p = k_0 a_p} = 0, \text{ with } p = 1, \ldots, N \tag{9}$$

$$\left[\frac{\partial}{\partial \rho_p}(V_i + V_r + V_s + V_{sr})\right]_{\rho_p = k_0 a_p} = 0, \text{ with } p = 1, \ldots, N \tag{10}$$

Substituting in (9) and (10) the expressions of the plane-wave fields V_i, and V_r, and the scattered field (5), and (8), and using the property of orthogonality satisfied by exponential functions, after some algebra it is possible to derive a linear system in the unknown coefficients c_{qm}:

$$\sum_{q=1}^{N} \sum_{m=-\infty}^{+\infty} A_{m\ell}^{qp(TM,TE)} c_{qm} = B_{\ell}^{p(TM,TE)} \quad \begin{cases} \ell = 0, \pm 1, \ldots, \pm\infty \\ p = 1, \ldots, N \end{cases} \tag{11}$$

with

$$\begin{aligned} A_{m\ell}^{qp(TM,TE)} &= i^{\ell} e^{-i\ell\varphi_i} G_{\ell}^{(TM,TE)}(\rho_p) \Big\{ CW_{m-\ell}(\xi_{qp}, \zeta_{qp}) \\ &\quad \times (1 - \delta_{qp}) + \frac{\delta_{qp}\delta_{\ell m}}{G_{\ell}^{(TM,TE)}(\rho_p)} \\ &\quad + RW_{m+\ell}(\chi_p + \chi_q, \eta_p - \eta_q) \Big\} \end{aligned} \tag{12}$$

$$\begin{aligned} B_{\ell}^{p(TM,TE)} &= -i^{\ell} e^{in_{\parallel}^{i}\eta_p} G_{\ell}^{(TM,TE)} \\ &\quad \times \{ e^{in_{\perp}^{i}\chi_p} e^{-im\varphi_i} + \Gamma_{01}(n_{\parallel}^{i}) \\ &\quad \times e^{-in_{\perp}^{i}\chi_p e^{-im\varphi_r}} \} \end{aligned} \tag{13}$$

where $\varphi_r = \pi - \varphi_i$, $G_{\ell}^{(TM)}(x) = J_{\ell}(x)/H_{\ell}^{(1)}(x)$ and $G_{\ell}^{(TE)} = J'_{\ell}(x)/H'^{(1)}_{\ell}(x)$.

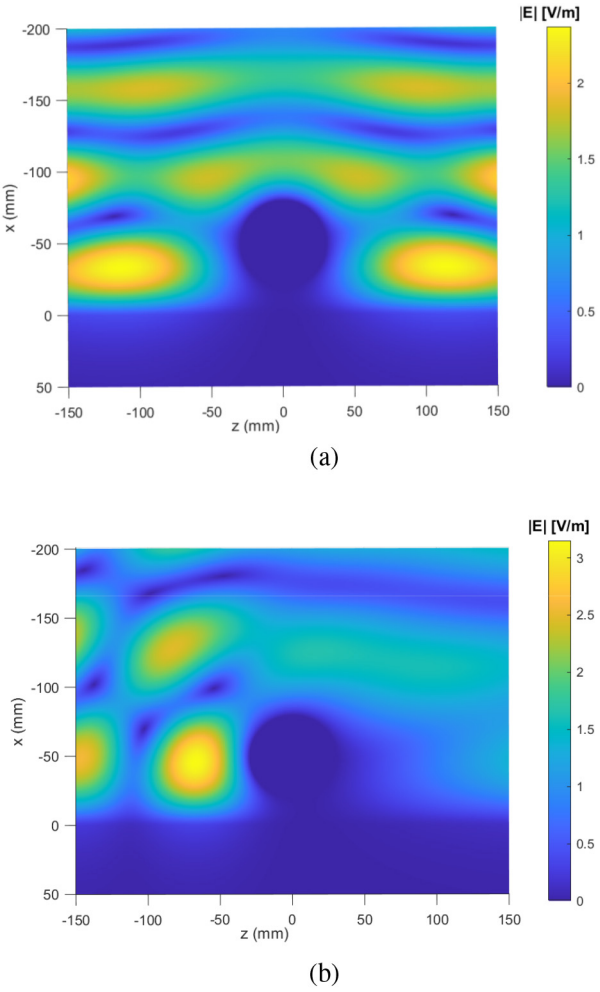

FIGURE 3. Magnitude of the total E-field on *xz*-plane (radius $a = 30$ mm, cylinder axis in $x = -50$ mm) for an incident field in TM polarization and: a) $\varphi_i = 0°$; b) $\varphi_i = 45°$.

III. NUMERICAL RESULTS

The CWA presented in Section II has been numerically implemented in a MATLAB code. In the numerical evaluation, a truncation is introduced on the order of cylindrical waves in (11). The criterion based on the properties of the Hankel functions suggested in [39] is applied, thus truncating the infinite series in (4), (5), and (8) between -M_t and +M_t with the rule $M_t = \lfloor 3\alpha_{MAX} \rfloor$, where α_{MAX} is the normalized radius of the largest cylinder.

The spectral integrals in (3) and (6) are solved in MATLAB, using the function `integral` that performs global adaptive quadrature [40]. The absolute tolerance was set to 10^{-5}, having an impinging wave of unitary amplitude.

In the numerical results, the application of the problem presented in Section II to the case of metallic targets below a biological medium is considered. In particular, a muscle is considered as filling medium of the lowest half-space, with permittivity $\varepsilon_{r1} = 52.8$ and electric conductivity $\sigma = 1.7$ S/m, at the frequency of ISM band $f = 2.4$ GHz. As to the excitation plane waves, unitary source fields are used, being 1 V/m the amplitude of the incident electric field in TM polarization, and 1 A/m the amplitude of the incident magnetic field in the TE one. Firstly, the case of a single perfectly conducting cylinder located above the muscle is considered. The cylinder has radius a=30 mm, and its axis lies 50 mm above the interface, centred on the z-axis. An impinging plane-wave, TM polarized, is in Medium 0 (vacuum). Two values of its incidence angle φ_i are considered, 0° and 45°. Figs. 3(a)–(b) show the magnitude of total E-field on the xz-plane, for $\varphi_i = 0°$ and 45°, respectively. It can be easily observed that in TM polarization the metallic cylinder has a shielding effect for the underlying region of Medium 1. The effect is shown clearly in Figs. 4(a)–(b), where the magnitude of the total E-field in the muscle of Fig. 3 is plotted along the $x = 30$ mm line, as a function of z, for $\varphi_i = 0°$ and 45°, respectively. To validate the CWA, results in Fig. 4 are compared with CST Microwave Studio [41], showing a very good agreement. Computation times for Fig. 4 are: CWA 42 s and CST 96 s. CWA computation was obtained with a truncation rule $M_t = 5$, while CST computation used 500.000 mesh elements. All computations were run on

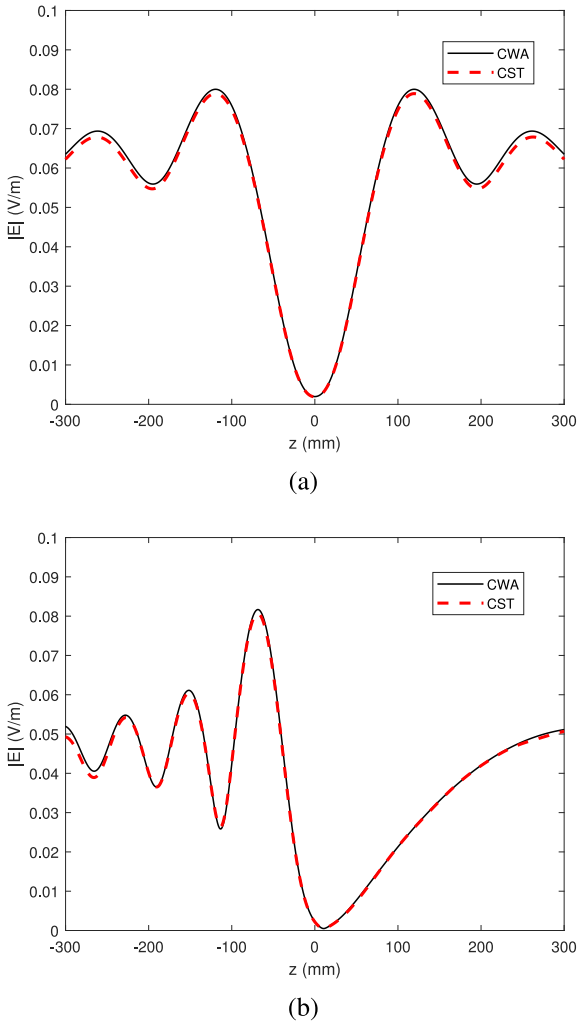

FIGURE 4. Magnitude of the total E-field in Fig. 3 along the line $x = 30$ mm in the muscle, compared with results from CST Microwave Studio: a) $\varphi_i = 0°$; b) $\varphi_i = 45°$.

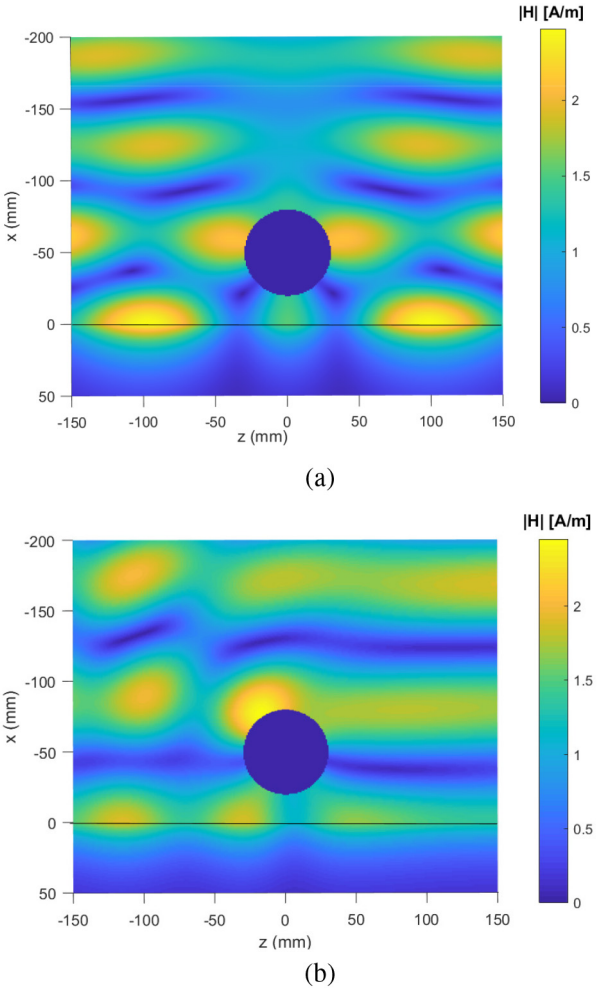

FIGURE 5. Magnitude of the total H-field on *xz*-plane (radius $a = 30$ mm, cylinder axis in $x = -50$ mm) for incident field in TE polarization and: a) $\varphi_i = 0°$; b) $\varphi_i = 45°$.

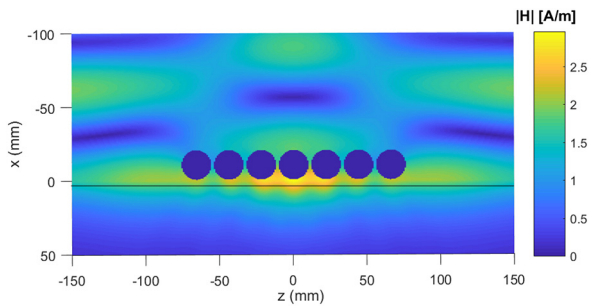

FIGURE 6. Magnitude of the total H-field on *xz* plane, in TE polarization and normal incidence ($\varphi_i = 0°$), with N=7 identical cylinders with radius $a_i = 10$ mm ($i = 1, \ldots, 7$). Cylinder axes aligned in $x = -11$ mm and center position are in $z = \{-68, -44, -22, 0, 22, 44, 68\}$ mm. Magnitude of the incident magnetic field is $|H| = 1$ A/m.

Intel i7-1065G7 @1.3 GHz processor, using 16 GB RAM. In case of large simulation domains, CST turns out to be much more time-consuming than CWA, as dense meshes are involved in the discretization. In the CWA, instead, the computational times are mainly determined by size of the targets and permittivity of the medium. In the CST simulation, a finite structure is modelled, bounded along the x and z-axes, and embedded in the y direction by two perfect electric walls parallel to the xz plane, when the impinging wave is TM polarized. In Fig. 5, the case of TE polarized wave is considered, in the same layout of Fig. 3, for $\varphi_i = 0°$ and 45°, respectively. The magnitude of the total H-field is reported on the xz-plane, showing the penetration of the H-field in the biological medium.

As a second case, a setup, having $N = 7$ cylinders in a symmetric configuration with respect to $z = 0$ plane, is considered. This is a setup that can be considered a simulation of a belt buckle on skin. The incident field is normally imping ($\varphi_i = 0°$) and in TE polarization. Cylinders have identical radii $a_i = 10$ mm ($i = 1, \ldots, 7$) and the horizontal distance between the axes of adjacent cylinders is 22 mm. All the cylinders are aligned parallel to the interface at $x = -11$ mm. In Fig. 6 the magnitude of the total H-field is reported, showing a good penetration in the muscle. As a further case, a layout similar to the one of Fig. 6 is considered; in particular the two layouts differ for the central cylinder, which now has a smaller radius $a_4 = 6$ mm, whereas $a_i = 10$ mm

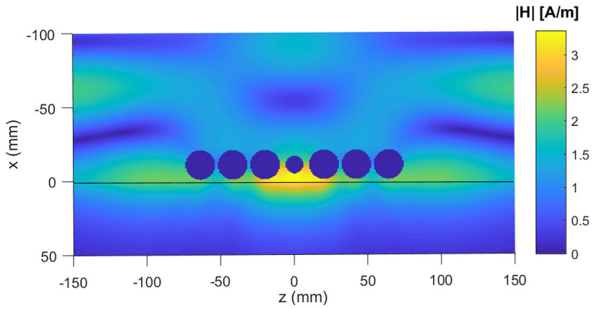

FIGURE 7. Magnitude of the total H-field on *xz* plane, in TE polarization and normal incidence ($\varphi_i = 0°$). Cylinders' radii are $a_i = 10$ mm ($i = 1, \ldots, 7, i \neq 4$), and $a_4 = 6$ mm. Cylinder axes aligned in $x = -11$ mm and center position are in $z = \{-64, -42, -20, 0, 20, 42, 64\}$ mm; $\varphi_i = 0°$.

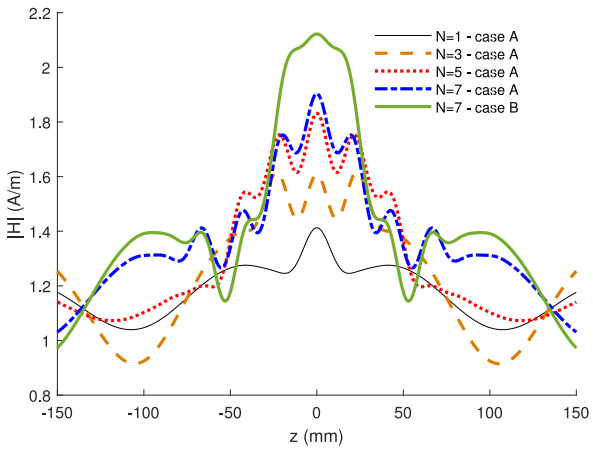

FIGURE 8. Magnitude of the total H-field along $x = 10$ mm line for the setup similar of Fig. 6 (Case A), for different values of the number of cylinders N, and the one of Fig. 7 (Case B).

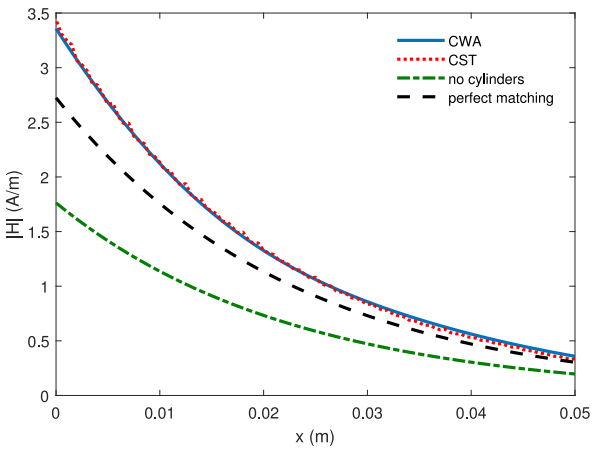

FIGURE 9. Magnitude of total H-field along $z = 0$ mm line for the same setup of Fig. 7. Comparison between CWA and CST, with cylinders. The case without cylinders, and adopting a layer that achieves a perfect match are also reported.

($i = 1, \ldots, 7, i \neq 4$). Results for this new setup are shown in Fig. 7: in this case the penetration of the H-field in the muscle is enhanced, if compared to the layout with identical cylinders of Fig. 6. The effect of the number of cylinders, for cylinders with identical radii, is shown in Fig. 8. In this plot

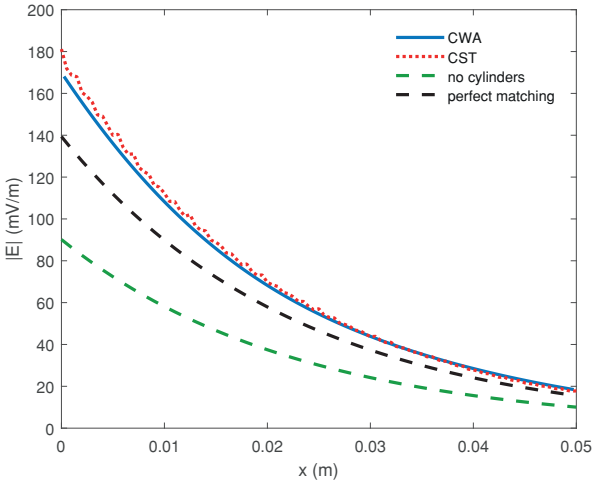

FIGURE 10. As in the Fig. 9 but for total E-field.

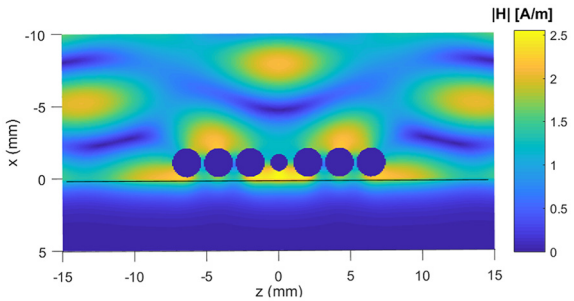

FIGURE 11. As in Fig. 7 but all geometrical parameters are scaled down by a factor 10, and at $f = 28$ GHz; $\varepsilon_{r1} = 24.44$ and $\sigma = 33.6$ S/m.

the total magnitude of the H-field in the muscle, along a line in $x = 10$ mm, is reported. It is shown how the magnitude of the total field is affected by an increased number of cylinders, with $N = 1, 3, 5, 7$. This case of cylinders with identical radii is labelled as 'Case A', and it is compared to the total H-field with $N = 7$, where the central cylinder has a smaller size, as in Fig. 7, labelled as 'Case B'. The enhancement of the H-field in the muscle introduced by the layout of 'Case B' can be fully appreciated.

With reference to the case B in Fig. 8, the field penetration along $z = 0$ line, as a function of x, is evaluated in Fig. 9 for the total magnetic field, and in Fig. 10, for the total electric field. Results including both the plane-wave fields and the scattered fields by the cylinders are compared to the field in absence of cylinders and adopting a layer that achieves a conjugate impedance matching (a layer on top of the muscle having the property of transmitting to the biological tissue all the incident power, acting as a quarter-wave transformer plus a reactive sheet that compensate the intrinsic inductance of the tissue). An interesting aspect of this configuration (Fig. 8 'case B'), which is in TE polarization, is that the cylinder array is able to intensify the electromagnetic field in the underlying region of the muscle, then it can be considered a favorable configuration for transmitting electromagnetic power to a possible

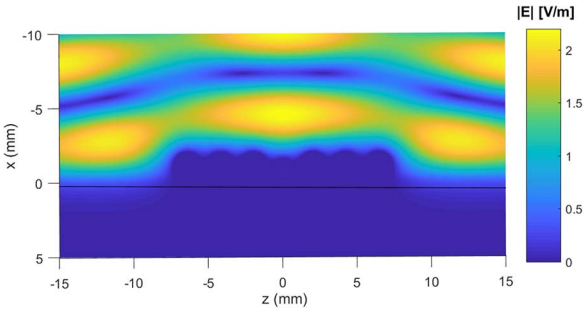

FIGURE 12. As in the Fig. 11 but for TM polarization.

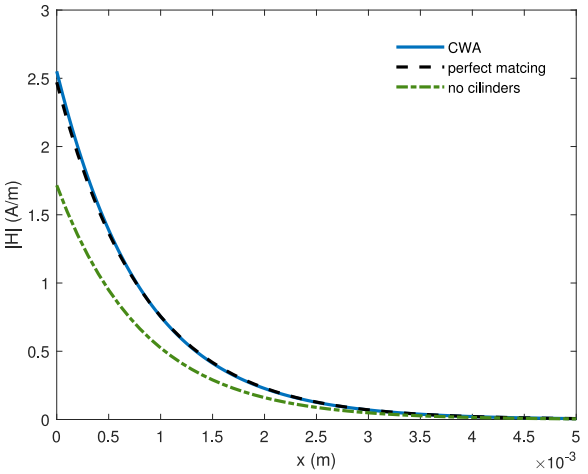

FIGURE 13. Magnitude of total H-field along z=0 mm line for the same setup of Fig. 11. The case without cylinders, and adopting a layer that achieves a perfect match are also reported for comparison.

implanted receiver. It is known [42] that an array of parallel conducting wires shows polarizing properties, where an intense scattering may be produced depending on the field polarization. In particular, TM-polarized fields undergo to a substantially more intense scattering by cylinders having axes parallel to the electric field [43]. This effect can be more or less intense depending on size, number of objects and the configuration. In the presented layout, the problem is complicated by the presence of the interface, due to different interactions in the reflection of the TM and TE polarizations.

A further case is the analysis of the geometrical layout as the one of Fig. 7, scaled to smaller dimensions, excited at $f = 28$ GHz to investigate field penetration in the millimeter band. Muscle parameters are, at this frequency of analysis, $\varepsilon_{r1} = 24.44$ and $\sigma = 33.6$ S/m. Results for TE polarization are presented in Fig. 11, and they still show a sub-subsurface penetration of the H-field. In the case of TM polarization, shown in Fig. 12, a strong shielding effect from the perfectly conducting cylinders is observed. With reference to the case of Fig. 11, the field penetration along z=0 line, is shown in Fig. 13 for the total magnetic field. In the same figure the results for no cylinders and for a layer that achieves a perfect matching impedance are also presented for comparison.

IV. CONCLUSION

In this article, a technique for the analytical solution to a problem of scattering by perfectly conducting cylinders above a semi-infinite and lossy medium has been presented. A plane-wave field has been considered as field source, and solution has been given in the cases of TM and TE polarizations. The problem has applications in evaluating the interaction of an electromagnetic field with a biological medium, when one or more metallic scatterers are placed above it.

In the numerical results, the biological medium has been modelled with a muscle, and the total field has been evaluated for different setups. The case of both a single cylinder and an alignment of cylinders have been shown. Simulations have been performed at a frequency of 2.4 GHz, and at the millimeter frequency of 28 GHz. The results have shown that, in TM polarization state, the metallic cylinders have a shielding effect on the penetration of the electric field in the muscle. In the TE state, instead, the magnetic field penetrates in the tissue, and in the presence of multiple scatteres such a penetration is even enhanced.

The method has not been yet applied to anisotropic scatterers. This generalization could be addressed by considering that in this case a coupling between polarizations must be taken into account, therefore a more extensive analytical and numerical study have to be introduced.

REFERENCES

[1] C. Liu, Y. Guo, H. Sun, and S. Xiao, "Design and safety considerations of an implantable rectenna for far-field wireless power transfer," *IEEE Trans. Antennas Propag.*, vol. 62, no. 11, pp. 5798–5806, Nov. 2014.
[2] K. Agarwal, R. Jegadeesan, Y.-X. Guo, and N. V. Thakor, "Wireless power transfer strategies for implantable bioelectronics," *IEEE Rev. Biomed. Eng.*, vol. 10, pp. 136–161, 2017.
[3] Z. Yang, L. Zhu, and S. Xiao, "An implantable wideband microstrip patch antenna based on high-loss property of human tissue," *IEEE Access*, vol. 8, pp. 93048–93057, 2020.
[4] K. Venugopal and R. W. Heath, "Millimeter wave networked wearables in dense indoor environments," *IEEE Access*, vol. 4, pp. 1205–1221, 2016
[5] T. Wu, T. S. Rappaport, and C. M. Collins, "Safe for generations to come: Considerations of safety for millimeter waves in wireless communications," *IEEE Microw. Mag.*, vol. 16, no. 2, pp. 65–84, Mar. 2015.
[6] F. Amato, C. Occhiuzzi, and G. Marrocco, "Epidermal backscattering antennas in the 5G framework: Performance and perspectives," *IEEE J. Radio Freq. Identification*, vol. 4, no. 3, pp. 176–185, Sep. 2020
[7] R. B. Green, M. Hays, M. Mangino, and E. Topsakal, "An anatomical model for the simulation and development of subcutaneous implantable wireless devices," *IEEE Trans. Antennas Propag.*, vol. 68, no. 10, pp. 7170–7178, Oct. 2020.
[8] S. Salous *et al.*, "Millimeter-wave propagation: Characterization and modeling toward fifth-generation systems," *IEEE Antennas Propag. Mag.*, vol. 58, no. 6, pp. 115–127, Dec. 2016.
[9] O. P. Gandhi and A. Riazi, "Absorption of millimeter waves by human beings and its biological implications," *IEEE Trans. Microw. Theory Techn.*, vol. 34, no. 2, pp. 228–235, Feb. 1986.
[10] J. E. Bjarnason, T. L. J. Chan, A. W. M. Lee, M. A. Celis, and E. R. Brown, "Millimeter-wave, terahertz, and mid-infrared transmission through common clothing," *Appl. Phys. Lett.*, vol. 85, no. 4, pp. 519–521, 2004.
[11] D. J. Daniels, *Surface Penetrating Radar*, 2nd ed. London, U.K.: IEE, 2004.
[12] M. G. Amin, *Through-the-Wall Radar Imaging*. New York, NY, USA: CRC Press, 2011.
[13] A. Q. Howard, "The electromagnetic fields of a subterranean cylindrical inhomogeneity excited by a line source," *Geophysics*, vol. 37, pp. 975–984, Dec. 1972.

[14] S. O. Ogunade, "Electromagnetic response of an embedded cylinder for line current excitation," *Geophysics*, vol. 46, pp. 45–52, Jan. 1981.
[15] S. F. Mahmoud, S. M. Ali, and J. R. Wait, "Electromagnetic scattering from a buried cylindrical inhomogeneity inside a lossy earth," *Radio Sci.*, vol. 16, no. 6, pp. 1285–1298, Nov./Dec. 1981.
[16] K. Hongo and A. Hamamura, "Asymptotic solutions for the scattered field of plane wave by a cylindrical obstacle buried in a dielectric half-space," *IEEE Trans. Antennas Propag.*, vol. 34, no. 11, pp. 1306–1312, Nov. 1986.
[17] L. Crocco, M. D'Urso, and T. Isernia, "The contrast source-extended born model for 2D subsurface scattering problems," *Progr. Elect. Res. B*, vol. 17, pp. 343–359, Sep. 2009.
[18] S.-C. Lee, "Scattering by a radially stratified infinite cylinder buried in an absorbing half-space," *J. Opt. Soc. Amer. A*, vol. 30, no. 4, pp. 565–572, Apr. 2013.
[19] C. Bourlier, N. Pinel, and G. Kubick, *Method of Moments for 2D Scattering Problems. Basic Concepts and Applications*. Hoboken, NJ, USA: Wiley, 2013.
[20] C. Li, D. Lesselier, and Y. Zhong, "Full-wave computational model of electromagnetic scattering by arbitrarily rotated 1-D periodic multilayer structure," *IEEE Trans. Antennas Propag.*, vol. 64, no. 3, pp. 1047–1060, Mar. 2016.
[21] M. A. Nasr, I. A. Eshrah, and E. A. Hashish, "Electromagnetic scattering from a buried cylinder using a multiple reflection approach: TM case," *IEEE Trans. Antennas Propag.*, vol. 62, no. 5, pp. 2702–2707, May 2014.
[22] A. S. Negm, I. A. Eshrah, and R. M. Badr, "Electromagnetic scattering from a buried cylinder using T-matrix and signal-flow-graph approach," in *Proc. EuCAP*, Lisbon, Portugal, Apr. 2015, pp. 1–4.
[23] X. Duan and M. Moghaddam, "Full-wave electromagnetic scattering from rough surfaces with buried inhomogeneities," *IEEE Trans. Geosci. Remote Sens.*, vol. 55, no. 6, pp. 3338–3353, Jun. 2017
[24] C. Ozzaim, "A perturbation method for scattering by a dielectric cylinder buried in a half-space," *IEEE Trans. Antennas Propag.*, vol. 66, no. 10, pp. 5662–5665, Oct. 2018.
[25] F. Frezza, L. Pajewski, C. Ponti, G. Schettini, and N. Tedeschi, "Electromagnetic scattering by a metallic cylinder buried in a lossy medium with the cylindrical wave approach," *IEEE Geosci. Remote Sens. Lett.*, vol. 10, no. 1, pp. 179–183, Jan. 2013.
[26] C. Ponti, M. Santarsiero, and G. Schettini, "Electromagnetic scattering of a pulsed signal by conducting cylindrical targets embedded in a half-space medium," *IEEE Trans. Antennas Propag.*, vol. 65, no. 6, pp. 3073–3083, Jun. 2017.
[27] M. A. Fiaz, F. Frezza, C. Ponti, and G. Schettini, "Electromagnetic scattering by a circular cylinder buried below a slightly rough Gaussian surface," *J. Opt. Soc. Amer. A*, vol. 31, no. 1, pp. 26–34, Jan. 2014.
[28] M. A. Fiaz, F. Frezza, L. Pajewski, C. Ponti, and G. Schettini, "Scattering by a circular cylinder buried under a slightly rough surface: The cylindrical-wave approach," *IEEE Trans. Antennas Propag.*, vol. 60, no. 2, pp. 2834–2842, Jun. 2012.
[29] F. Frezza, L. Pajewski, C. Ponti, and G. Schettini, "Scattering by perfectly conducting circular cylinders buried in a dielectric slab through the cylindrical wave approach," *IEEE Trans. Antennas Propag.*, vol. 57, no. 4, pp. 1208–1217, Apr. 2009.
[30] F. Frezza, L. Pajewski, C. Ponti, and G. Schettini, "Through-wall electromagnetic scattering by N conducting cylinders," *J. Opt. Soc. Amer. A*, vol. 30, no. 8, pp. 1632–1639, Aug. 2013.
[31] C. Ponti and S. Vellucci, "Scattering by conducting cylinders below a dielectric layer with a fast non-iterative approach," *IEEE Trans. Microw. Theory Tech.*, vol. 63, no. 1, pp. 30–39, Jan. 2015.
[32] E. Porter, M. Coates, and M. Popovic, "An early clinical study of time-domain microwave radar for breast health monitoring," *IEEE Trans. Biomed. Eng.*, vol. 63, no. 3, pp. 530–539, Mar. 2016.
[33] I. Bisio *et al.*, "Brain stroke microwave imaging by means of a Newton-conjugate-gradient method in L^p banach spaces," *IEEE Trans. Microw. Theory Tech.*, vol. 66, no. 8, pp. 3668–3682, Aug. 2018.
[34] R. Borghi, F. Gori, M. Santarsiero, F. Frezza, and G. Schettini, "Plane-wave scattering by a perfectly conducting circular cylinder near a plane surface: Cylindrical-wave approach," *J. Opt. Soc. Amer. A*, vol. 13, no. 3, pp. 483–493, Mar. 1996.
[35] R. Borghi, F. Frezza, M. Santarsiero, C. Santini, and G. Schettini, "A quadrature algorithm for the evaluation of a 2D radiation integral with a highly oscillating kernel," *J. Electromagn. Waves Appl.*, vol. 14, no. 10, pp. 1353–1370, 2000.
[36] G. Cincotti, F. Gori, M. Santarsiero, F. Frezza, F. Furnò, and G. Schettini, "Plane wave expansion of cylindrical functions," *Opt. Commun.*, vol. 95, pp. 192–198, Jan. 1993.
[37] R. Borghi, F. Frezza, P. Oliverio, M. Santarsiero, and G. Schettini, "Scattering of a generic two-dimensional field by cylindrical structures in the presence of a plane interface," *J. Infrared Mil. Terahertz Waves*, vol. 21, no. 5, pp. 805–827, 2000.
[38] I. N. Sneddon, *Mixed Boundary Value Problems in Potential Theory.* Amsterdam, The Netherlands: North-Holland, 1966.
[39] A. Z. Elsherbeni, "A comparative study of two-dimensional multiple scattering techniques," *Radio Sci.*, vol. 29, pp. 1023–1033, Jul./Aug. 1994.
[40] L. F. Shampine, "Vectorized adaptive quadrature in MATLAB," *J. Comput. Appl. Math.*, vol. 211, no. 2, pp. 131–140, 2008.
[41] *CST Microwave Studio Suite 2020*. [Online]. Available: https://www.3ds.com/products-services/simulia/products/cst-studio-suite/
[42] Y. Zhou and D. Klotzkin, "Design and parallel fabrication of wire-grid polarization arrays for polarization-resolved imaging at 1.55 μm," *Appl. Opt.*, vol. 47, no. 20, pp. 3555–3560, 2008.
[43] C. A. Balanis, *Advanced Engineering Electromagnetics*. Hoboken, NJ, USA: Wiley, 2012.

CRISTINA PONTI (Member, IEEE) received the Laurea (*cum laude*) and Laurea Magistralis (*cum laude*) degrees in electronic engineering from the Sapienza University of Rome in 2004 and 2006, respectively, and the Ph.D. degree in March 2010. In 2006, she joined the Applied Electronics Department, Roma Tre University, Rome, Italy, where from November 2006 to October 2009 she attended the Doctoral School in Biomedical Engineering, Electromagnetism, and Telecommunications. Since December 2010, she has been an Assistant Professor in Electromagnetic Fields. Her main research interests are in electromagnetic analysis, scattering problems, buried-objects detection, ground penetrating radar, through-the-wall radar, numerical methods, electromagnetics-bandgap materials, antennas, and microwave components for high-power applications. She was a Co-Convener of conference sessions at URSI EMTS 2016, URSI EMTS 2019, and URSI GASS 2021. She is an Associate Editor of *IET Microwaves, Antennas and Propagation*. She is a Member of the IEEE Antennas and Propagation and Women in Engineering Societies, National Interuniversity Consortium for Telecommunications, amd Italian Society of Electromagnetics.

LUDOVICA TOGNOLATTI (Graduate Student Member, IEEE) was born in Rome, Italy, in April 1994. She received the B.S. and M.S. degrees (*cum laude*) in electronic engineering from Roma Tre University, Rome, in 2017 and 2019, respectively, where she is currently pursuing the Ph.D. degree with the Section of Applied Electronics, Department of Engineering. Her current research interests include periodic structures, numerical methods, leaky-wave antennas, and electromagnetic scattering.

GIUSEPPE SCHETTINI (Senior Member, IEEE) received the Laurea degree (*cum laude*) in electronic engineering, the Ph.D. degree in applied electromagnetics, and the Laurea degree (*cum laude*) in physics from the La Sapienza University of Rome, Rome, Italy, in 1986, 1991, and 1995, respectively. Upon his graduation in electronic engineering, he joined the Italian Energy and Environment Agency, where he was initially involved with free electron generators of millimeter waves and then on microwave components and antennas for heating of thermonuclear plasmas. In 1992, he joined La Sapienza University as a Researcher of electromagnetics. In 1998, he joined the Department of Engineering, Section of Applied Electronics, Roma Tre University of Rome, Rome, where he was an Associate Professor from 1998 to 2005, and a Full Professor of Electromagnetic Fields since 2005. From 2013 to 2017, he was the Deputy Director for Research with the Department of Engineering. He is currently the Rector's delegate for North America technology transfer. His scientific research is focused on structures for guiding and radiation of electromagnetic fields for microwave and millimeter waves applications, scattering, diffractive optics, plasma heating and current drive, electromagnetic band gap media, and anisotropic media. He is an Associate Editor of the IEEE OPEN JOURNAL OF ANTENNAS AND PROPAGATION. He is a member of several scientific and technical societies in the frame of information technology, in particular in the field of electromagnetic systems. He is also a member of the editorial boards and technical program committes of several international journals and conferences in the field of microwaves and antennas.